PROJECTILE FRAGMENTATION AND ISOTOPIC SCALING IN A TRANSPORT APPROACH*

T.I. Mikhailova[a], B. Erdemchimeg[a,b], A.G. Artukh[a]
M. Di Toro[c], H.H. Wolter[d]

[a]JINR, Dubna, Moscow region, 141980, Russia
[b]National University of Mongolia, 210646 Ulaanbaatar, Mongolia
[c]LNS — INFN, 95125 Catania CT, Italy
[d]University of Munich, 80539 Munich, Germany

(Received January 23, 2017)

We investigate projectile fragmentation using transport theory coupled with statistical decay codes for the excited primary fragments. We concentrate on isotope distributions and on an isoscaling analysis of isotope ratios to obtain information about the symmetry energy. The analysis is performed depending on the impact parameter since the thermodynamic properties of the primary fragments depend on it strongly. We compare reaction systems with different neutron and proton excess, ^{38}Ar, ^{40}Ca+^{9}Be and ^{48}Ca, ^{40}Ca+^{9}Be both at 140 AMeV, to investigate the range of validity of the isoscaling assumption. We find it is well-justified for isotopes which are mainly produced by the secondary decay. However, for isotopes with N or Z near the incident projectile for grazing impact parameters, the process is more direct and the distributions are not well-represented by statistical ensembles. In the range of validity, the extracted symmetry energies are generally reasonable.

DOI:10.5506/APhysPolBSupp.10.121

1. Introduction

Fragmentation in nuclear collisions of light heavy-ion projectiles continue to be of very actual interest [1]. It is of practical importance in the production of new species of neutron-rich exotic nuclei, and generally in applications in accelerator driven technologies in medicine and waste treatment. Therefore, there are many efforts to better understand fragmentation.

Fragmentation depends sensitively on the incident energy, impact parameter and the reaction system. A very useful characterization is possible by a representation introduced by Wilczyński [2], which displays in effect

* Presented at the XXIII Nuclear Physics Workshop "Marie and Pierre Curie", Kazimierz Dolny, Poland, September 27–October 2, 2016.

the total energy loss *versus* the deflection angle in an essentially binary reaction. An example is given in Fig. 1 for three reactions of light heavy ions on ^{9}Be targets in the Fermi energy range from 30 to 140 AMeV, which have been studied by us in the past [3, 4]. At low energies, ^{18}O shows the typical characteristics of a deep-inelastic collision with orbiting and strong dissipation. At the upper Fermi energy range of 140 AMeV, one observes more an abrasion–ablation-type process, where part of the projectile is cut away by the target and the residual nucleus is highly excited depending on the impact parameter. At 50 AMeV, one is somewhere in the middle. In the present article, we discuss the reactions of several projectiles at the higher energy on Be targets.

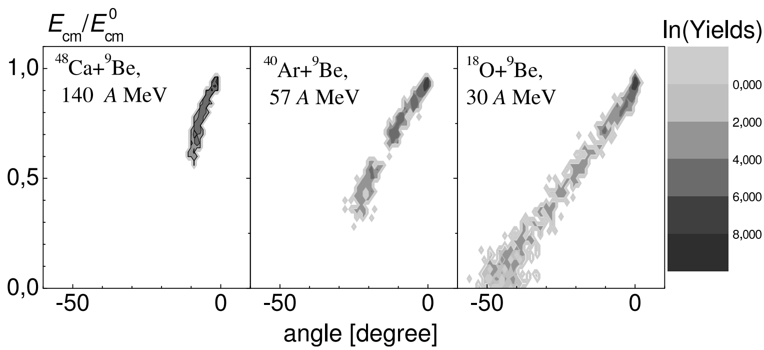

Fig. 1. The Wilczyński plot of the ratio of final and initial kinetic energies *versus* the deflection angle of the residual projectile fragment for different projectiles at different incident energies. The contour plot shows the yields of the residual fragment obtained from transport calculations [3, 4].

There is a range of theoretical approaches to describe fragmentation. Widely used are phenomenological, semi-phenomenological, or statistical models, which are generally very successful to predict fragmentation patterns, such as the EPAX, DIT, HIPSE or Goldhaber abrasion models [5] which, however, depend on adjusted phenomenological parameters. On the other hand, microscopic approaches, in particular transport theories, follow the evolution of the one-body phase space distribution taking into account two-body collisions. There are two variants of such theories, Boltzmann-like theories (usually named Boltzmann–Uehling–Uhlenbeck (BUU) or Boltzmann–Nordheim–Vlasov (BNV) models), and molecular dynamics approaches (usually called Quantum Molecular Dynamics models (QMD)). The microscopic approaches have the advantage that they describe all aspects of the evolution and are, in principle, free of parameters adjusted to the process.

Here, we use the BNV approach which we have used previously to describe fragmentation reactions at lower energies from the Coulomb barrier to the Fermi energy [3]. There we discussed not only isotope yields but also velocity or energy spectra of the fragments. These are found to be very sensitive to the mechanism and also more difficult to explain. We will not discuss them here but in further work.

Recently, one has studied the isotope yields of pairs of reactions, which differ with respect to their isospin. Ratios of isotopic yields can give information on the nuclear symmetry energy, which is defined by an expansion of the energy per nucleon in terms of the asymmetry of the system as $E(\rho, \delta) = E_{\rm nm}(\rho) + E_{\rm sym}(\rho)\delta^2 + \ldots$, where $\delta = (\rho_n - \rho_p)/\rho$, and the ρs are the respective partial and total densities. $E_{\rm nm}(\rho)$ and $E_{\rm sym}(\rho)$ are the energy of symmetric nuclear matter and the symmetry energy, respectively. The symmetry energy is of particular interest today, because of its poor theoretical knowledge and the importance in many fields of nuclear and astrophysics [6]. Quantitatively, this analysis is done by the isoscaling method introduced by Tsang *et al.* [7]. For the reaction pair ^{40,48}Ca+^{9}Be, ^{181}Ta, it was measured and analyzed in Ref. [8] and also in Refs. [4, 9]. The large difference in neutron content for the ^{40,48}Ca pair introduces some particular behavior. Therefore, we compare it here to the more similar reaction pair ^{38}Ar, ^{40}Ca+^{9}Be. A particular feature of the study of Ref. [4] and here is that the isoscaling analysis is done depending on the impact parameter of the reaction, which allows to more closely control such properties of the produced fragments as the excitation energy and isospin.

2. Transport approach and fragmentation

As mentioned above, we use the BNV approach to model the nuclear collision and the fragmentation process, which cannot be explained here in any detail. A standard reference to the method is Ref. [10]. In Ref. [4], we review in compact form the methods used here. The BNV method describes the time evolution of the one-body phase space distribution in a nuclear collision under the influence of a self-consistent mean field, and a two-body collision term, which takes into account two-body dissipation via an effective in-medium cross section and respects the Pauli principle.

The collision is followed until the freeze-out state, where the interactions between the fragments cease. In the energy region considered here, the final state in the projectile region consists of a large "primary" fragment and several small particles, which represent the ejected "gas". The primary fragment is excited and will go through a subsequent statistical decay. This takes a long time and is usually not described dynamically but with the help of statistical decay codes. In our case, we used the Statistical Multifragmentation Model (SMM) by Bondorf *et al.* [11]. For this code, the mass and charge of the primary fragment and its excitation energy need to be specified. In our approach, we calculate the excitation energy using the same mean field as in the transport code and comparing with the ground state energy calculated in the same way of a nucleus with the same N, Z of the fragment. In Fig. 2, we show the average mass, charge, and excitation energy per nucleon of the primary fragment as a function of the impact parameter for the three reactions. One sees that the size of the fragment decreases and the excitation energy, and thus also the temperature increases with smaller impact parameters as expected. Thus, the fragments cannot be treated globally by statistical ensembles. Therefore, in the following, we will analyze the isospin scaling depending on the impact parameter.

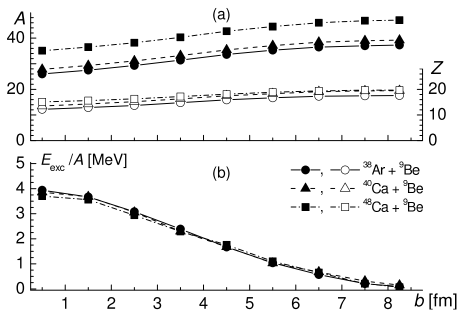

Fig. 2. (a) Average mass, charge, and (b) excitation energy per nucleon of the primary fragments as a function of impact parameter for the reactions identified in the legend at 140 AMeV.

3. Results

3.1. Isotope distributions

We have performed calculations for collisions of the reaction systems ^{38}Ar, ^{40}Ca and ^{48}Ca on the target ^{9}Be at 140 MeV per nucleon. We investigate the isotope yields and the isoscaling ratios for ^{48}Ca–^{40}Ca and ^{38}Ar–^{40}Ca. The first system was already investigated in Ref. [4], however the results differ slightly here due to different constraints in the evaluation as explained below. In Ref. [4], we concentrated on the comparison with the experiment, which was also performed for the system ^{48}Ca–^{40}Ca in Refs. [8,9]. Here, we are mainly interested in comparing the behavior of two systems which differ considerably by the neutron excess. An important point in Ref. [4] was to consider the yields and ratios depending on the impact parameter b, since, as discussed above, the thermodynamic properties of the primary fragments depend strongly on it. Thus, we often discuss results selected according to impact parameter bins between 0 and 8 fm. The sums of the radii of the three systems are between 6.5 and 6.8 fm.

In Fig. 3, we show the yields for the three reactions as contour plots for a central impact parameter bin on the left- and a peripheral one on the right-hand side; in each case for the primary fragments of the BNV calculation and after the secondary de-excitation using SMM. It is evident that the

BNV distributions are much narrower and also much more symmetric than the ones after de-excitation. The SMM distributions display a long tail of lighter isotopes due to evaporation of nucleons and light clusters. This effect is stronger for the low impact parameter because of the larger excitation energy. Secondly, one sees that the distributions for ^{38}Ar and ^{40}Ca overlap rather well, but, as expected, the ones for ^{48}Ca are much more shifted to the neutron-rich side, less so, for the small impact parameter. At a close look, one sees also a smaller shift in Z of ^{38}Ar relative to ^{40}Ca.

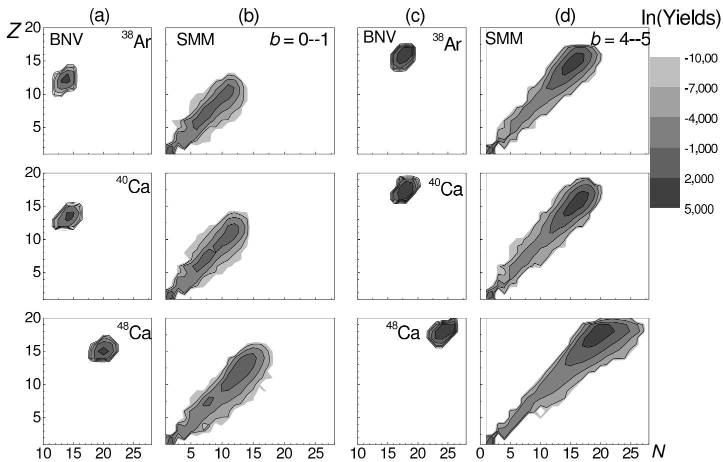

Fig. 3. Yields (nat. log.) of the reactions ^{38}Ar, ^{40}Ca, and ^{48}Ca on ^{9}Be at 140 AMeV (top to bottom rows), presented as contour plots in the plane of N and Z. The columns (a) and (b) show the yields in the impact parameter bin of 0 to 1 fm, columns (c) and (d) for 4 to 5 fm; columns (a) and (c) the yields of the primary fragments of the BNV calculation, and columns (b) and (d) the yields after the secondary de-excitation using the SMM code.

These effects will be important when studying ratios of isotope yields for two reactions as it is done in an isoscaling analysis. For $b = 4$ to 5 fm, yields for ^{48}Ca for neutron numbers around $N = 20$ are large, while for the same neutron numbers, the yields for ^{40}Ca are either non-existing or very small. An analogous effect is still seen for the small impact parameter. Thus, ratios of yields for such isotopes are very large. They are not very meaningful in an isoscaling analysis, because the isotopes arise from very different situations which cannot be considered as coming from comparable statistical ensembles. The same is true to a lesser degree with respect to charge number for the comparison of ^{38}Ar and ^{40}Ca. In the isoscaling analysis, we will therefore omit very large or very small values of the ratios.

3.2. Isoscaling and the symmetry energy

In the isoscaling analysis, one considers ratios of yields of isotopes in two reactions 1 and 2 of different isospin content of the colliding nuclei

$$R_{21} = \frac{Y_2(N,Z)}{Y_1(N,Z)} \equiv C \exp\left(\alpha(Z)N + \beta(N)Z\right). \tag{1}$$

These ratios often display an exponential behavior as a function of N or Z of the isotope. When assuming that the isotopes are emitted from a system described by a grand canonical ensemble of common temperature T, the isoscaling parameters α and β are given as differences of the neutron and proton chemical potentials as $\alpha = \Delta\mu_n/T$ and $\beta = \Delta\mu_p/T$. Then the isoscaling coefficients can be directly related to the symmetry energy as

$$\alpha = \frac{4F_{\rm sym}}{T}\left[(Z/A)_1^2 - (Z/A)_2^2\right] \tag{2}$$

and correspondingly for β. Here, $F_{\rm sym}(\rho,T)$ is the symmetry free energy of the emitting system of density ρ and temperature T.

In Fig. 4, we show a contour plot in the (N,Z) plane of the isotope yield ratios according to Eq. (1) for the two reaction systems for impact parameters 0 to 1 fm (upper row) and 4 to 5 fm (lower row). If isoscaling according to Eq. (1) was strictly obeyed, then the equi-ratio lines in this plot were regularly spaced straight lines. It is seen that this is rather well-obeyed for large parts of the occupied area in the (N,Z) plane. The increase of the ratios is rather for $N+Z=$ constant in the direction of larger N, *i.e.* for more neutron rich isotope pairs. Note that because of this, α is positive and β negative.

Howerver, this behavior is not seen everywhere. For the ^{48}Ca–^{40}Ca pair, there are very large values and strong deviations from the linear behavior for isotopes with large N and Z. This is related to the relative shifts of the isotope distributions which were discussed in connection with Fig. 3 at the end of the last subsection. Similar, though not as drastic, effects are seen for the ^{38}Ar–^{40}Ca pair for large Z values, this time with very small values of the ratio (because now the lighter nucleus is in the numerator). Not only are the values of the ratios very large or small, but also the parallel lines are strongly distorted. The isoscaling coefficients are determined by a cut through this graph for fixed Z or N, and a linear fit to the corresponding curve. Where the lines are distorted, this cut is not a linear relation any more, and thus the determination of isoscaling coefficients is not meaningful.

The isoscaling coefficients determined from the plot of Fig. 4 are displayed in Fig. 5 as contour plots in the plane (b,Z), respectively (b,N), for the reaction ^{38}Ar and ^{40}Ca on ^{9}Be in panels (a), (b), and for ^{48}Ca and ^{40}Ca on ^{9}Be in panels (c), (d). For large areas, these coefficients are rather

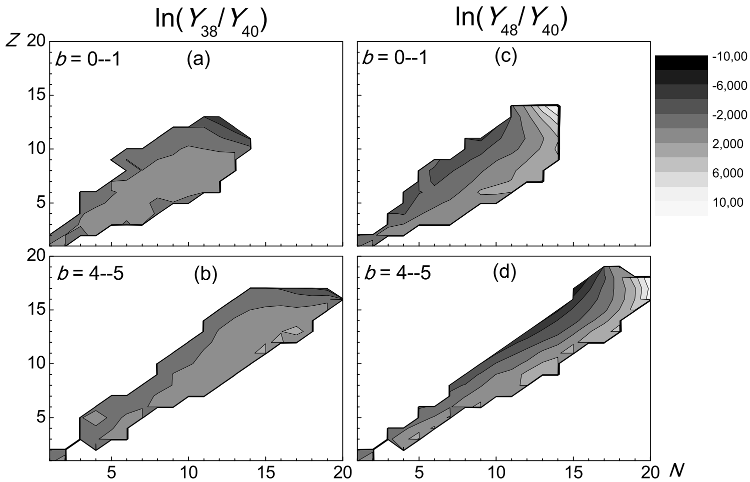

Fig. 4. Contour plot of the yield ratios (nat. log.) of isotopes in the (N, Z) plane for the reactions ^{38}Ar and ^{40}Ca on ^{9}Be (panels (a), (b)) and ^{48}Ca and ^{40}Ca on ^{9}Be (c), (d) for impact parameters 0 to 1 fm (a), (c) and 4 to 5 fm (b), (d).

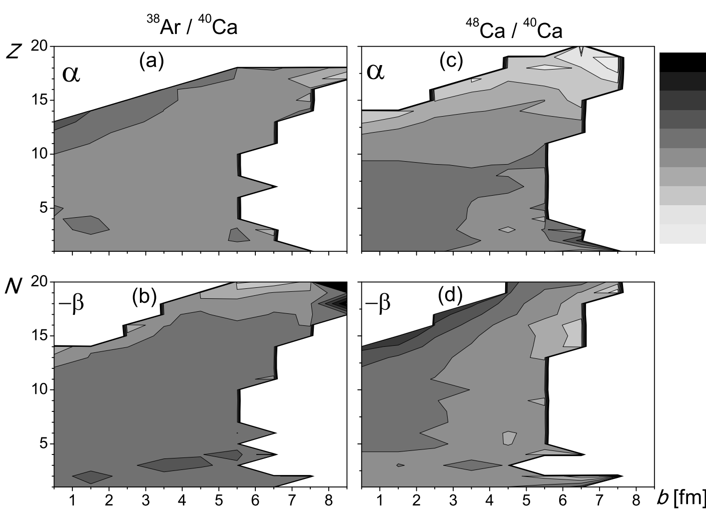

Fig. 5. Contour plot of the isoscaling coefficients α (panels (a), (c)) and $-\beta$ (b), (d) for the reactions ^{38}Ar and ^{40}Ca on ^{9}Be (a), (b) and ^{48}Ca and ^{40}Ca on ^{9}Be (c), (d) in the plane of impact parameters and Z for α, respectively N for β.

constant as expected from the isoscaling assumption. However, at the upper edge and particularly in the upper right corner, *i.e.* for large impact parameters and isotopes close to the projectile, the values are very large or very small, especially for the ^{48}Ca–^{40}Ca pair, as expected from the ratios in Fig. 4. Thus, isoscaling is well-satisfied in regions, where the isotope distributions are dominated by the statistical decay of the primary fragments. In regions where the fragments are close to the projectile, the character of the reaction is more direct and the isotopic scaling is not applicable. By projecting these contour plots onto the Z or N axes, *i.e.* integrating over impact parameter b with weights taking into account the yields of the two reactions in the ratio, one can compare with the common way of applying isoscaling without consideration of the impact parameter, and also compare to experiment. This was done for the ^{48,40}Ca on ^{9}Be reactions in Ref. [4] with the result of a rather good agreement between the three ways of determining isoscaling coefficients. This will have to be investigated more generally.

In order to derive the symmetry energy according to Eq. (2), we have to average $\alpha(Z)$ over Z and $\beta(N)$ over N. This is done separately for each impact parameter bin. According to the arguments given above, we do this only for those regions where the isoscaling parameters are reasonably constant. We have chosen the interval [0,1] for the ^{38}Ar–^{40}Ca system and [0,2] for ^{48}Ca–^{40}Ca, but this is, of course, somewhat arbitrary. These averaged values are given as a function of impact parameter in the upper panel of Fig. 6 for the two reaction systems. It is seen that α and β are rather close in absolute value in each system, but they differ for the two systems. It is seen that in spite of the above constraint in the averaging, the values at the largest impact parameters are still not reliable.

We now apply Eq. (2). The differences in the average Z/A and N/A ratios, respectively, can be taken for each impact parameter bin from Fig. 2. We connect in a rather approximate way the excitation energy with the temperature with a Fermi gas-like expression $T^2 = c\,E_{\mathrm{exc}}/A$ with c usually in the range from 8 to 13 MeV and with $c = 10$ MeV used here. The resulting values for the symmetry free energy are shown in the lower panel of Fig. 6 for the two systems for the symmetry energy derived from the isoscaling coefficients α and β, respectively, as a function of impact parameter or temperature (upper abscissa). The symmetry energies as a function of temperature are seen to agree with each other fairly well. They are approximately constant for impact parameters up to about 5–6 fm. Beyond, they decrease probably due to the reasons discussed above with respect to the inapplicability of the assumption of a grand canonical ensemble. The value of around 25 MeV seems reasonable when considering that the primary fragment has a density lower than saturation density. In addition, there are expected to be entropic effects in going from the free to the internal symmetry energy, which need to be further investigated.

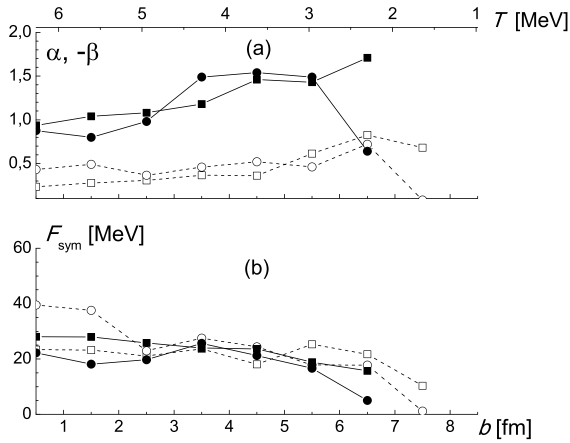

Fig. 6. (a) Averaged isoscaling coefficients α (squares) and $-\beta$ (circles) as a function of impact parameter for the reaction pairs ^{48}Ca, ^{40}Ca+^{9}Be (solid lines, full symbols) and ^{38}Ar, ^{40}Ca+^{9}Be (dashed lines, open symbols). (b) Symmetry free energy derived from the isoscaling coefficients (same signatures). A temperature scale corresponding to the impact parameters is given at the top.

4. Summary

We compared projectile fragmentation of different light heavy ion projectiles on ^{9}Be at an energy in the upper range of Fermi energies, where the nature of the process changes from deep-inelastic to an abrasion picture. For the investigation, we used a Boltzmann-type transport theory together with a statistical decay code, which allows to get a detailed view of the mechanism. We represent the results as contour plots of isotope yields and related quantities, from which we obtain a good global view of the process. We aimed to compare projectiles of different neutron or proton excess with each other, and not necessarily with experiment, which was done in previous work. The analysis is performed depending on the impact parameter since the projectile fragment is changing strongly in mass, charge and excitation energy, *i.e.* also temperature, as a function of impact parameter.

The results on the isotope yields are used to investigate the symmetry energy with the isoscaling method by studying isotopic yield ratios for two reaction pairs, one with a large neutron excess (^{48}Ca–^{40}Ca) and one which is more similar (^{38}Ar–^{40}Ca). In the contour plots of the ratios, we see that these have an exponential behavior in large regions of the isotopic landscape, signifying that a thermodynamic approach as assumed by the isoscaling method is valid. But there are also regions of large impact parameters and/or N and Z close to the projectile, where the ratios behave very differently, due to the more direct nature of the collision, which cannot be described by thermodynamics. It will have to be investigated further, how this affects the standard methods of applying isoscaling to determine the symmetry energy. Finally, we extract the symmetry energy in the regions of validity. We obtain values of the symmetry energy which vary little with temperature and are below those generally accepted at saturation density due to the fact that the primary fragments have lower densities.

This work was supported by the Heisenberg–Landau program of the DFG, Germany and JINR, Russia, and partly by the Universe Excellence Cluster of the DFG, Germany. T.M. would like to thank the organizing committee of the XXIII Nuclear Physics Workshop for the hospitality and the fruitful atmosphere.

REFERENCES

[1] S. Momota *et al.*, *Phys. Rev. C* **92**, 024608 (2015).

[2] J. Wilczyński, *Phys. Lett. B* **47**, 484 (1973).

[3] T.I. Mikhailova *et al.*, *Rom. J. Phys.* **52**, 875 (2007); *Bull. Russ. Acad. Sci.* **73**, 852 (2009); *Int. J. Mod. Phys. E* **19**, 678 (2010); *Bull. Russ. Acad. Sci.* **75**, 1511 (2011); *Part. Nucl. Lett.* **12**, 646 (2015).

[4] T.I. Mikhailova *et al.*, *Phys. At. Nucl.* **79**, 604 (2016).

[5] K. Sümmerer, *Phys. Rev. C* **86**, 014601 (2012); M. Veselsky *et al.*, *Nucl. Phys. A* **781**, 521 (2007); D. Lacroix *et al.*, *Phys. Rev. C* **69**, 054604 (2004); A.S. Goldhaber, *Phys. Lett. B* **53**, 306 (1974).

[6] B.A. Li *et al.* (eds.), *Eur. Phys. J. A* **50**, 9 (2014); C.J. Horowitz *et al.*, *J. Phys. G: Nucl. Part. Phys.* **41**, 093001 (2014).

[7] M.B. Tsang *et al.*, *Phys. Rev. Lett.* **86**, 5023 (2001); *Phys. Rev. C* **64**, 041603 (2001).

[8] M. Mocko *et al.*, *Phys. Rev. C* **78**, 024612 (2008).

[9] Y. Fu *et al.*, *Chin. Phys. Lett.* **26**, 082503 (2009).

[10] G.F. Bertsch, S. Das Gupta, *Phys. Rep.* **160**, 189 (1988).

[11] P. Bondorf *et al.*, *Phys. Rep.* **257**, 133 (1995).